Cellular and Molecular Neurobiology (2021) 41:115–127
https://doi.org/10.1007/s10571-020-00839-w

ORIGINAL RESEARCH

# Evodiamine Inhibits Lipopolysaccharide (LPS)-Induced Inflammation in BV-2 Cells via Regulating AKT/Nrf2-HO-1/NF-κB Signaling Axis

**Tianyu Meng[2] · Shoupeng Fu[1] · Dewei He[1] · Guiqiu Hu[1] · Xiyu Gao[1] · Yufei Zhang[1] · Bingxu Huang[1] · Jian Du[1] · Ang Zhou[1] · Yingchun Su[1] · Dianfeng Liu[1]**

Received: 30 October 2019 / Accepted: 1 April 2020 / Published online: 11 April 2020


## Abstract

Neuroinflammation is caused by excessive activation of microglia and plays an essential role in neurodegenerative diseases. After activation, microglia produce several kinds of inflammatory mediators, trigger an excessive inflammatory response, and ultimately destroy the surrounding neurons. Therefore, agents that inhibit neuroinflammation may be potential drug candidates for neurodegenerative diseases. Evodiamine (EV) has anti-inflammatory functions in peripheral tissues. However, whether EV exerts the same function in neuroinflammation is not known. In the present study, the aim was to explore whether EV attenuates microglial overactivation and therefore suppresses the development of neuroinflammation in lipopolysaccharide (LPS)-stimulated BV-2 cells. It was found that EV effectively inhibited expression of proinflammatory mediators (cyclooxygenase-2 (COX-2), inducible nitric oxide synthase (iNOS), interleukin-6 (IL-6), and tumor necrosis factor-α (TNF-α)) via AKT/Nrf2/HO-1 activation and suppressed NF-κB p65 phosphorylation. In addition, EV could suppress LPS-induced inflammatory response and loss of dopaminergic neuron in mouse mesencephalic neuron--glia cells. Hence, these findings demonstrate that EV suppresses neuroinflammation caused by overactivated microglia via regulating the AKT/Nrf2/HO-1/NF-κB signaling axis.

**Keywords** Evodiamine · Microglia · Neuroinflammation · Neurodegenerative disease

## Abbreviations

| | |
|---|---|
| EV | Evodiamine |
| LPS | Lipopolysaccharide |
| AKT | Protein kinase B |
| Nrf2 | Nuclear factor erythroid 2-related factor 2 |
| HO-1 | Heme oxygenase-1 |
| NF-κB | Nuclear transcription factor-κB |

Tianyu Meng, Shoupeng Fu, Dewei He, and Guiqiu Hu have contributed equally to this work.

✉ Dianfeng Liu
ccldf@163.com

Tianyu Meng
mengty9916@mails.jlu.edu.cn

Shoupeng Fu
fushoupeng@jlu.edu.cn

Dewei He
m13144303829@163.com

Guiqiu Hu
guiqiuhu@jlu.edu.cn

Xiyu Gao
gaoxy9916@mails.jlu.edu.cn

Yufei Zhang
zhangyf9916@mails.jlu.edu.cn

Bingxu Huang
huangbingxu123@163.com

Jian Du
jiandu18@mails.jlu.edu.cn

Ang Zhou
zhouang9918@mails.jlu.edu.cn

Yingchun Su
suyc9918@mails.jlu.edu.cn

[1] College of Animal Science and Veterinary Medicine, Jilin University, Changchun, China

[2] College of Food Science and Engineering, Jilin University, Changchun, China

## Introduction

Neurodegenerative disease is a general term for chronic progressive central nervous system diseases that feature the degeneration and loss of primary neuronal cells and includes Alzheimer's disease (AD), Parkinson's disease (PD), and Huntington's disease (HD) (Jewett et al. 2017; Khanam et al. 2016). Causes of neurodegenerative diseases are still not well understood, and it is generally believed that they are closely associated with heredity, inflammation, apoptosis, oxidative stress, mitochondrial dysfunction, and so on(Liddelow et al. 2017; Norden et al. 2015; Spires-Jones et al. 2017). Numerous studies have recently indicated that neuroinflammation arising from microglial overactivation plays a vital role in the pathogenesis of neurodegenerative diseases (Hirsch and Hunot 2009; Miklossy et al. 2006; Mrvova et al. 2015). Upon activation, microglia release proinflammatory mediators (inducible nitric oxide synthase (iNOS), cyclooxygenase-2 (COX-2), tumor necrosis factor-α (TNF-α), and interleukin-6 (IL-6)), which damage surrounding neurons (Hurley et al. 2003; Rosa et al. 2018). Neuronal damage signals further activate microglia. Therefore, inhibiting the inflammatory microglial response will be beneficial for neurodegenerative disease therapy.

Evodiamine (EV) is a natural alkaloid and a primary biologically active ingredient of *Evodia rutaecarpa*, a medicinal plant used in traditional Chinese medicine (Hu et al. 2017). Pharmacological studies have shown that EV binds to a variety of proteins, and so it can be used as a multitarget compound for tumors, obesity, pain, inflammation, cardiovascular disease, and Alzheimer's disease (Cai et al. 2014; Wang et al. 2013; Wu et al. 2013; Yu et al. 2013). It has been reported that EV plays specific anti-inflammatory roles in cardiovascular and cerebrovascular diseases (e.g., atherosclerosis (Wei et al. 2013)), gastrointestinal diseases (e.g., stomach ulcer (Zhao et al. 2015) and colorectal cancer (Zhou et al. 2019)), and tumorigenesis (e.g., lung cancer(Mohan et al. 2016) and ovarian cancer (Wei et al. 2016)). However, there is currently no research on the role of EV in neuroinflammation. It was hypothesized that EV inhibits neuroinflammation mediated by overactivation of microglia. Hence, this research provides a novel view of the role of EV in anti-inflammatory responses, which in turn provides a potential therapeutic approach for neuroinflammation.

## Results

### Effect of EV on BV-2 Cell Viability

To evaluate the toxicity of EV, the survival rates of BV-2 cells (after EV treatment) were measured by CCK-8 assay. After culturing the cells with different doses of EV and CCK-8 solution, the cell suspension was collected to measure the optical density (at 450 nm). No significant change was found in optical density in the group incubated with EV (2.5 μM, 5 μM, 10 μM, and 20 μM) or its solvent DMSO compared to that of the control group. Therefore, EV at the chosen concentration did not impact BV-2 cell viability (Fig. 1).

### EV Inhibits the Production of Proinflammatory Factors and Proinflammatory Enzymes in LPS-Stimulated BV-2 Cells

It was hypothesized that EV exerts an anti-inflammatory effect in an induced neuroinflammation cell model. To validate this hypothesis, it was first explored whether EV inhibits the production of proinflammatory mediators. The cell suspension was collected using TRIzol reagent to analyze the mRNA levels of proinflammatory mediators by quantitative real-time PCR. Under LPS stimulation, the mRNA levels of proinflammatory cytokines showed rapid increase

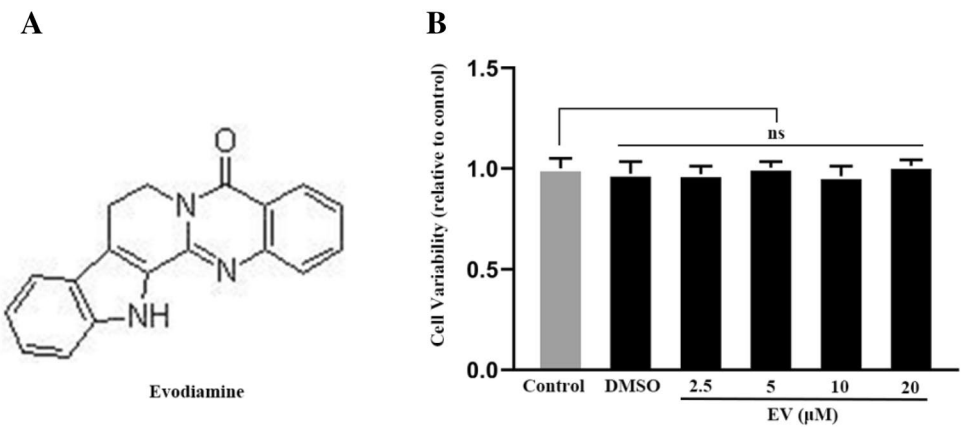


**Fig. 1** **a** Chemical structure of evodiamine (EV). **b** Effect of EV on cell viability. After pretreatment with different concentrations of EV and its solvent DMSO, the viability of BV-2 cells was detected by a CCK-8 kit. All data are expressed as the mean ± SEM

(increased by 74,736.18% in IL-6, 26,036.08% in TNF-α, 49,094.27%, in iNOS, and 4786.68% in COX-2, respectively, as shown in Fig. 2a–d). It was found that EV reduced the LPS-induced gene expression of proinflammatory mediators (10 μM EV reduced gene expression to 66.42% in IL-6, 73.13% in TNF-α, 70.92% in iNOS, and 53.24% in COX-2 compared to LPS-induced groups). 20 μM EV reduced gene expression to 50.47%, 65.55%, 54.62%, and 49.82%, respectively, as shown in Fig. 2a–d). Moreover, the protein levels of proinflammatory cytokines (IL-6, TNF-α) and enzymes (COX-2 and iNOS) were screened by Western blotting and ELISA. It was found that EV also reduced the expression of proinflammatory cytokines at the protein level (LPS stimulation upregulates protein levels to 74,007.30% in IL-6, 28,486.27% in TNF-α, 2154.70% in iNOS, and 777.32% in COX-2. 10 μM EV reduced protein expression to 42.34% in IL-6,74.99% in TNF-α, 49.82% in iNOS, and 57.44% in COX-2, respectively; 20 μM EV reduced it to 16.15%, 29.28%, 51.94%, and 54.29%, respectively, as shown in Fig. 2e–i).These results suggest that EV prevented the secretion of proinflammatory mediators, which further demonstrates that EV inhibits inflammation in LPS-stimulated BV-2 cells (Fig. 2).

## EV Suppresses NF-κB Pathway Activation in LPS-Stimulated BV-2 Cells

Many molecules that are involved in the inflammatory response are regulated by the NF-κB pathway. IκB α is an inhibitor of NF-κB. In the cytoplasm, NF-κB is not activated, and it is bound to IκBα. LPS activates IKK (IκB kinase), and activated IKK ubiquitinates, phosphorylates,

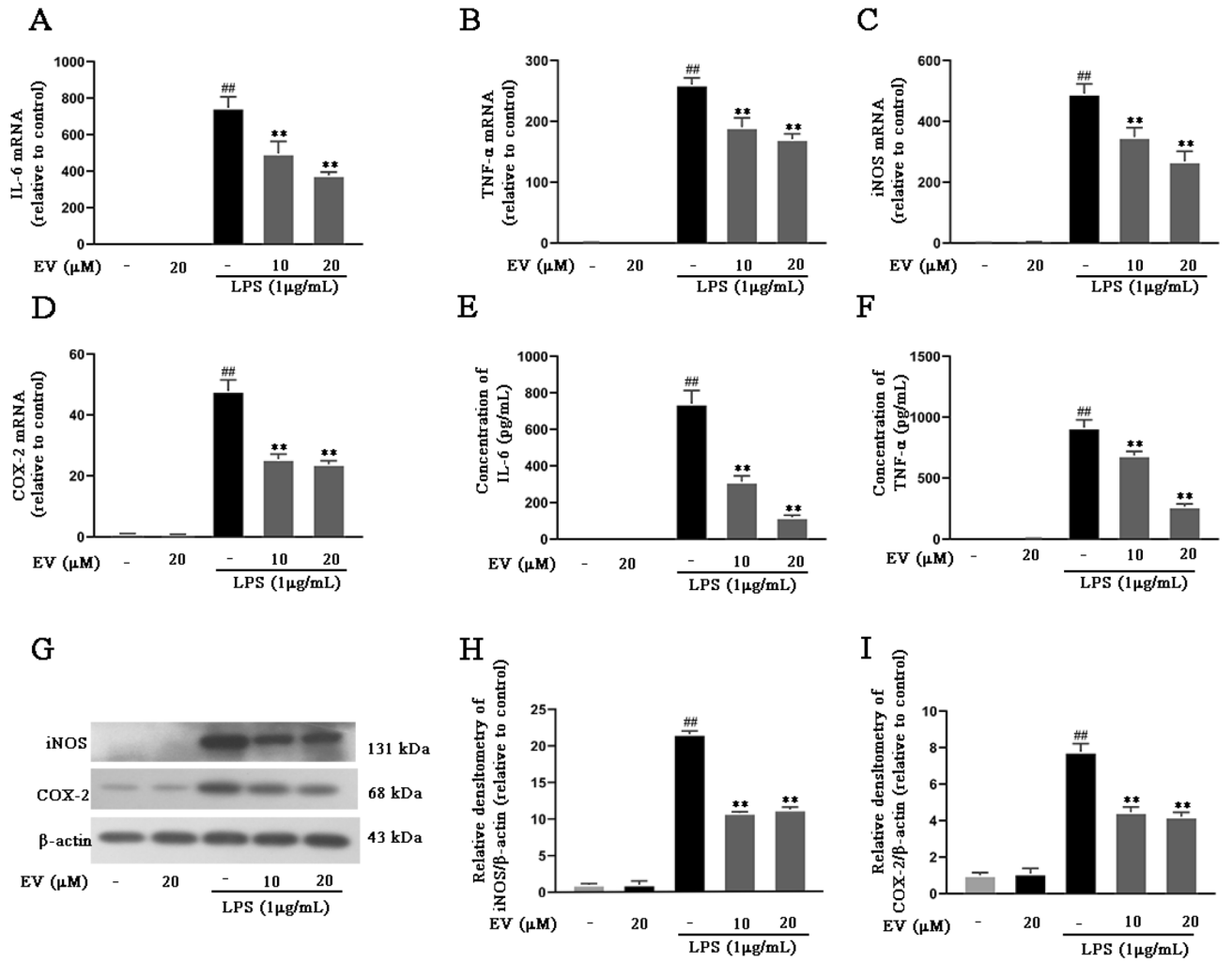


**Fig. 2** eV treatment inhibiting the production of proinflammatory mediators. BV-2 cells were pretreated with EV (10 μM and 20 μM) for 1 h and then exposed to LPS (1 μg/mL) for 6 h. The mRNA levels were quantified by quantitative real-time PCR. The protein levels were examined by Western blotting or ELISA. Blots were analyzed by ImageJ. The values are presented as the mean ± SEM ($n = 5$ in each level). $^{\#\#}p < 0.01$ compared to the untreated group. $^{**}p < 0.01$ versus the LPS-treated group

and degrades IκBα, which activates NF-κB and transfers it into the nucleus (specifically the p65 subunit), where NF-κB binds with the promoters of inflammation-associated genes, initiates inflammatory mediator transcription, and induces an inflammatory response. The molecular mechanism was further investigated by detecting the effects of EV on IκBα degradation and NF-κB p65 and IκBα phosphorylation. LPS stimulation reduced IκBα to 25.87%, upregulated p-IκBα (809.09%) and p-NF-κB p65 (445.93%) compared to the control. EV inhibited LPS-mediated IκBα degradation (EV10: 196.24%, EV20: 268.21%), the phosphorylation of IκBα (EV10: 88.19%, EV20: 51.49%), and NF-κB p65 (EV10: 57.60%, EV20: 40.88%), further indicating that EV plays an anti-inflammatory role by suppressing activation of the NF-κB signaling pathway (Fig. 3).

## EV Promotes the Phosphorylation of AKT, Enhances Intracellular Localization of Nrf2, and Upregulates HO-1 Expression in BV-2 Cells

Previous studies have indicated that the Nrf2, HO-1, and AKT pathways are involved in inflammation. To further verify the anti-inflammatory mechanism of EV, the AKT, Nrf2, and HO-1 signaling pathways were investigated after EV (20 μM) treatment at different times (0, 0.5, 1, 3, and 6 h). Western blotting showed that EV promoted AKT phosphorylation, enhanced the nuclear translocation of Nrf2, and upregulated the expression of HO-1 (Fig. 4).

## EV Promotes Nuclear Translocation of Nrf2 via the AKT Signaling Pathway in BV-2 Cells

Previous studies have illustrated that Nrf2 activation is regulated by upstream kinases. To confirm that EV treatment regulates Nrf2 nuclear translocation by the AKT pathway, BV-2 cells were pretreated with MK2206 (an AKT inhibitor, 10 μM) and then stimulated the cells with EV (20 μM). The expression of phospho-AKT, nuclear Nrf2 (Nu-Nrf2), and cytoplasmic Nrf2 (Cy-Nrf2) was detected by Western blotting. The results indicated that MK2206 pretreatment suppressed EV-induced nuclear translocation of Nrf2, which was mediated by the AKT pathway (Fig. 5).

## EV Upregulates HO-1 Expression by Activating the Nrf2 Pathway in BV-2 Cells

To illustrate the relationship between HO-1 and Nrf-2, BV-2 cells were pretreated with RA (an inhibitor of Nrf2, 5 μM) for 4 h and then incubated with EV (20 μM) for 3 h. Then, the protein levels of HO-1 and Nu-Nrf2 were measured. The results indicated that the protein levels of HO-1 and Nu-Nrf2 increased considerably in the EV-treated group compared to those of the untreated group (Fig. 6). As expected, the inhibition of Nrf2 abolished the EV-induced upregulation of HO-1 protein (Fig. 6a, c). In addition, RA treatment alone did not affect the protein levels of HO-1 or Nu-Nrf2 (Fig. 6). Overall, these results showed that EV upregulated HO-1

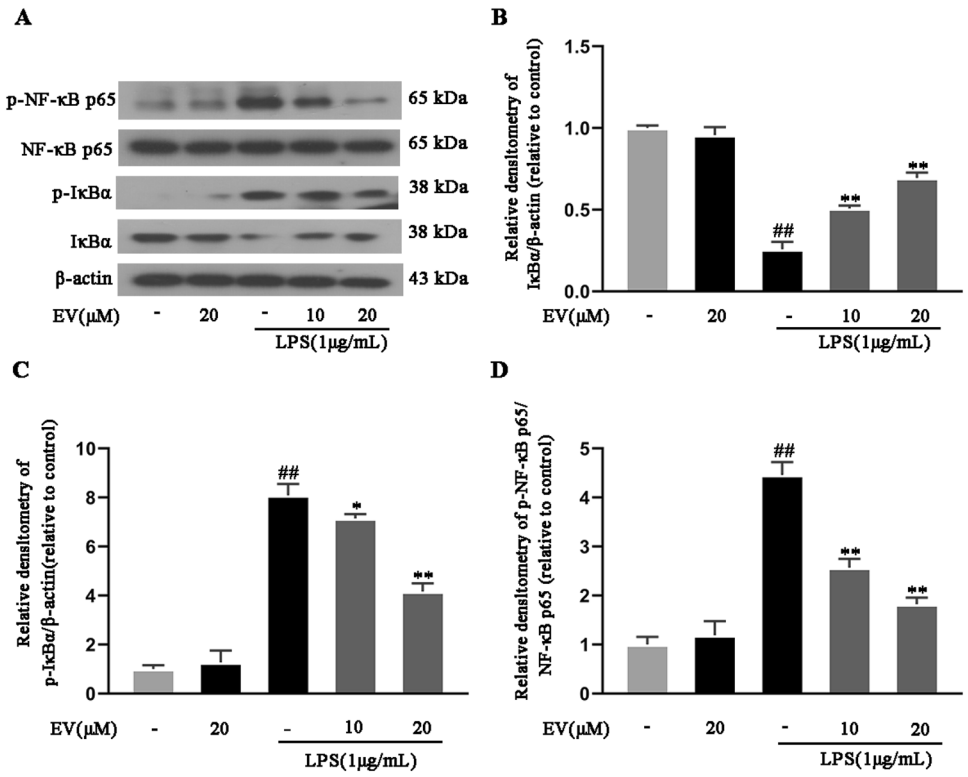


**Fig. 3** eV suppressing activation of the NF-κB pathway in LPS-stimulated BV-2 cells. BV-2 cells were pretreated with EV (10 μM and 20 μM) for 1 h and then stimulated with LPS for 1 h. Total proteins were collected using lysis buffer. The protein levels and phosphorylated forms of IκB and NF-κB p65 were examined by Western blotting. The values are shown as the mean ± SEM ($n = 5$ in each group). $^{\#\#}p < 0.01$ compared to the untreated group. $^{*}p < 0.05$ and $^{**}p < 0.01$ versus the LPS-treated group

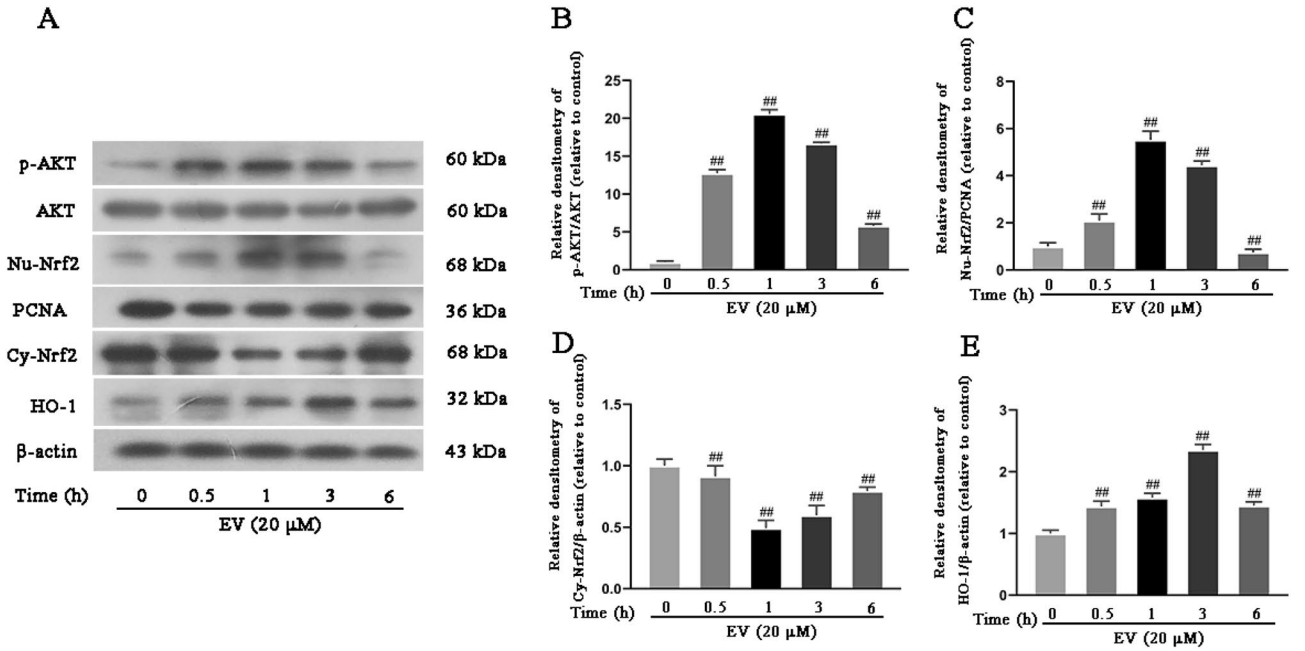


**Fig. 4** Effect of EV treatment on the AKT, Nrf2, and HO-1 pathways. BV-2 cells were treated with or without EV (20 μM) for 0.5, 1, 3, and 6 h. Protein levels of nuclear Nrf2 (Nu-Nrf2), phospho-AKT, HO-1, and cytoplasmic Nrf2 (Cy-Nrf2) were examined via Western blotting. β-actin was used as an internal reference, and PCNA was used as a nuclear internal standard. The values are shown as the mean ± SEM ($n = 5$ in each group). $^{\#\#}p < 0.01$ compared to the untreated group

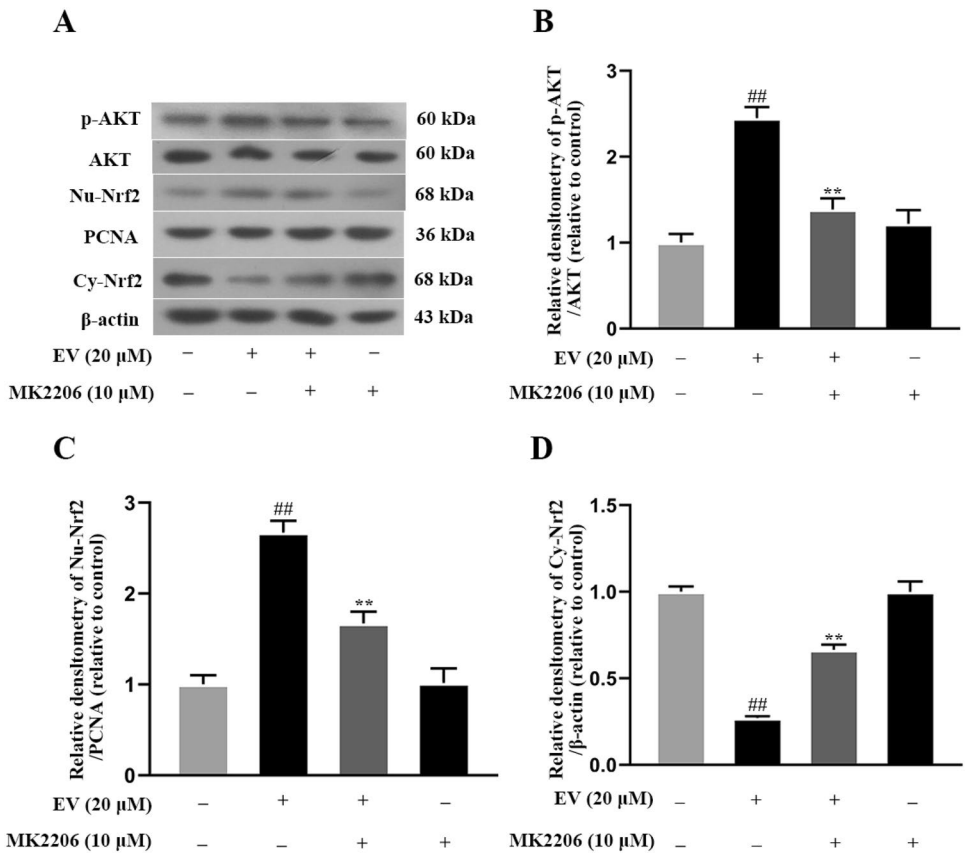


**Fig. 5** eV promoting the nuclear translocation of Nrf2 via the AKT signaling pathway. BV-2 cells were pretreated with MK2206 (an inhibitor of AKT, 10 μM) and then treated with EV (20 μM) for 1 h. Protein levels of Nu-Nrf2, Cy-Nrf2, and phospho-AKT were detected by Western blotting. The values are presented as the mean ± SEM ($n = 5$ in each group). $^{\#\#}p < 0.01$ compared to the untreated group. $^{**}p < 0.01$ versus the EV-treated group

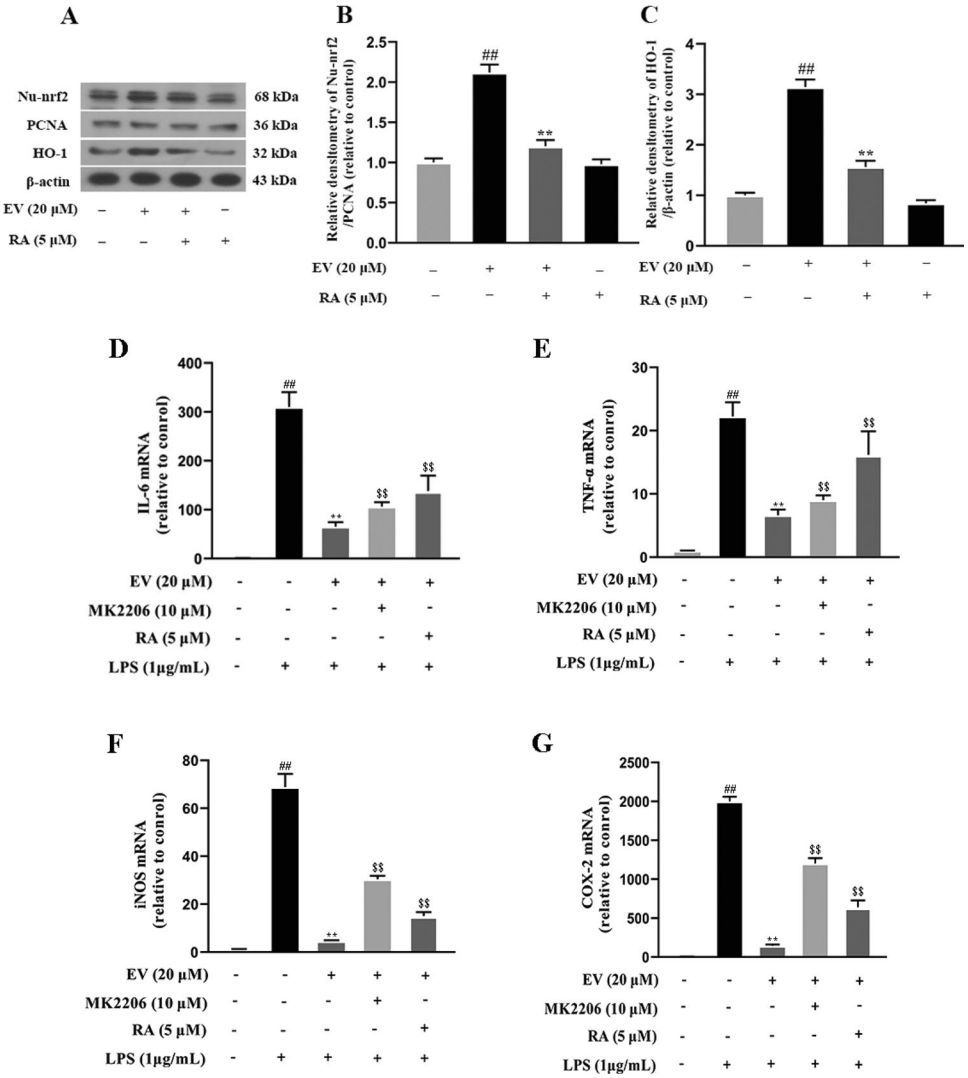


**Fig. 6** **a–c** EV upregulating HO-1 expression by activating the Nrf2 pathway. After exposed to RA (an inhibitor of Nrf2, 5 μM) for 4 h, BV-2 cells were treated with EV (20 μM) for 3 h. Then, the levels of Nu-Nrf2 and HO-1 were detected by Western blotting. **d–g** After exposed to MK2206 (10 μM) for 4 h, BV-2 cells were treated with EV (20 μM) for 1 h and then stimulated with LPS (1 μg/mL) for 6 h. The mRNA levels of IL-6, TNF-α, iNOS, and COX-2 were analyzed using quantitative real-time PCR. All above indicated that RA and MK2206 pretreatment partially abolished effect of EV on inhibiting the production of proinflammatory mediators. The values are presented as the mean ± SEM ($n = 5$ in each group). $^{\#\#}p < 0.01$ compared to the untreated group. $^{**}p < 0.01$ versus the EV-treated group. $^{\$\$}p < 0.01$ versus the EV + LPS-treated group

expression by activating the Nrf2 pathway. Furthermore, it was examined whether RA and MK2206 pretreatment affected the anti-inflammatory function of EV. It was found that RA and MK2206 pretreatment partially abolished the effect of EV on inhibiting the production of proinflammatory mediators (COX-2, iNOS, IL-6 and TNF-α) in BV-2 cells (Fig. 6d–g). The production of proinflammatory mediators increased in LPS group (IL-6: 31,013.09%, TNF-α: 2227.04%, iNOS: 6890.72%, and COX-2: 200,083.37%). EV + LPS group alleviated the secretion to 21.12% (IL-6), 29.80% (TNF-α), 6.64% (iNOS), and 7.25% (COX-2) compared to LPS group. After MK2206 blocking, the production rapidly increased to 162.44% in IL-6, 135.95% in TNF-α, 665.11% in iNOS, and 829.74% in COX-2 compared to LPS + EV group. Similarly, RA blocking upregulates the secretion to 210.89%, 243.94%, 329.51%, and 441.67%, respectively. These results confirmed that EV inhibited the inflammatory phenotype via the AKT/Nrf-2 pathway in LPS-stimulated BV-2 cells.

## EV Inhibits Activation of the NF-κB Pathway and Production of Proinflammatory Mediators via the HO-1 Pathway in LPS-Stimulated BV-2 Cells

Studies have indicated that HO-1 regulates the NF-κB pathway. Furthermore, it was examined whether pretreatment with SnPP IX (an inhibitor of HO-1, 40 μM) affects the anti-inflammatory function of EV. The results showed that SnPP IX pretreatment decreased the inhibitory effect of EV on NF-κB p65 phosphorylation and the production of proinflammatory mediators (COX-2, iNOS, IL-6, and TNF-α) in BV-2 cells. The production of proinflammatory mediators increased in LPS group (IL-6: 3121.49%, TNF-α: 2863.70%, iNOS: 8484.49%, and COX-2: 4167.23%). EV + LPS group alleviated the secretion to 49.82% (IL-6), 55.61% (TNF-α), 54.72% (iNOS), and 63.10% (COX-2) compared to LPS group. After SnPP-IX blocking, the production rapidly increased to 155.84% in IL-6, 121.03% in TNF-α, 134.08% in iNOS, and 127.35% in COX-2 compared to LPS + EV

group (Fig. 7c–f). These results suggest that EV inhibits NF-κB pathway activation and the production of proinflammatory mediators via the HO-1 pathway in LPS-stimulated BV-2 cells (Fig. 7).

## EV Treatment Increases the Number of Tyrosine Hydroxylase (Th)-Positive Cells and Inhibits the Inflammatory Response in Primary Mouse Mesencephalic Neuron--Glia Cells

LPS-induced primary mesencephalic neuron--glia cells were used to study on the protection of anti-inflammatory substances on dopaminergic neurons. In order to clarify whether EV protects neurons via inhibiting neuroinflammation, the loss of TH (biological markers of dopaminergic neurons)-positive cells and the inflammatory response were examined in LPS-induced primary mouse mesencephalic neuron--glia cells. LPS reduced the number of dopaminergic neurons to 54.80%. The results showed that EV attenuated LPS-induced increase of gene expression of proinflammatory mediators (IL-6, TNF-α, iNOS, and COX-2) (Fig. 8a–d) and the loss of TH-positive cells (the number of dopaminergic neurons was up to 145.26% compared to LPS-stimulated group, as shown in Fig. 8f) in mesencephalic neuron--glia cells. In addition, the process of TH-positive cells became shorter and even deformed

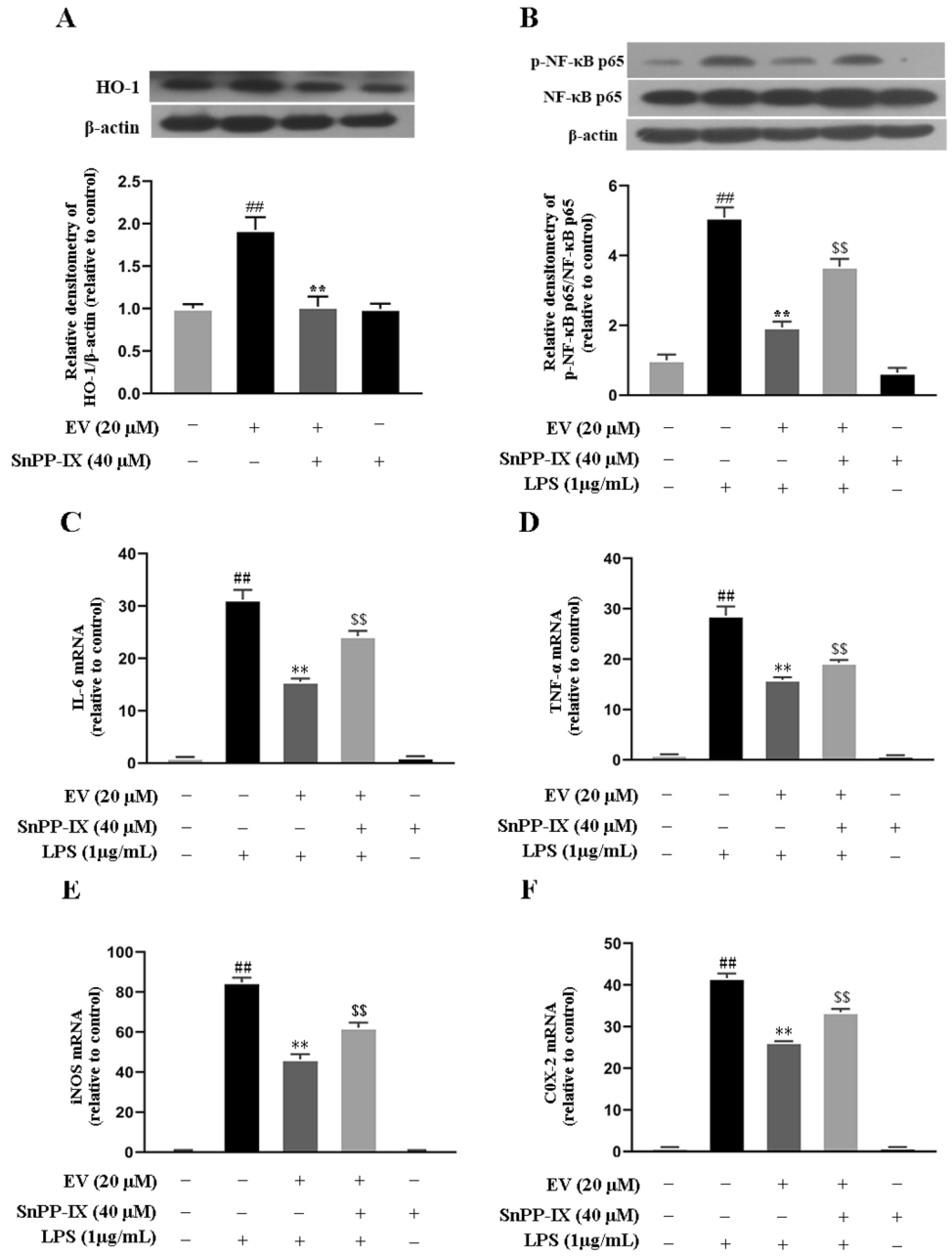


**Fig. 7** eV inhibiting activation of the NF-κB pathway and the production of proinflammatory mediators via the HO-1 pathway in LPS-stimulated BV-2 cells. BV-2 cells were pretreated with SnPP-IX (an inhibitor of HO-1, 40 μM) for 3 h, treated with EV (20 μM) for 1 h, and stimulated with LPS (1 μg/mL) for 6 h (mRNA) or 1 h (protein). Protein levels of phospho-NF-κB p65 and HO-1 were detected by Western blotting. The expression proinflammatory mediators (COX-2, iNOS, IL-6, and TNF-α) were measured using quantitative real-time PCR. β-actin was used as an internal control. The values are presented as the mean ± SEM ($n = 5$ in each group). $^{\#\#}p < 0.01$ compared to the untreated group. $^{**}p < 0.01$ versus the LPS-treated group. $^{\$\$}p < 0.01$ versus the EV + LPS-treated group

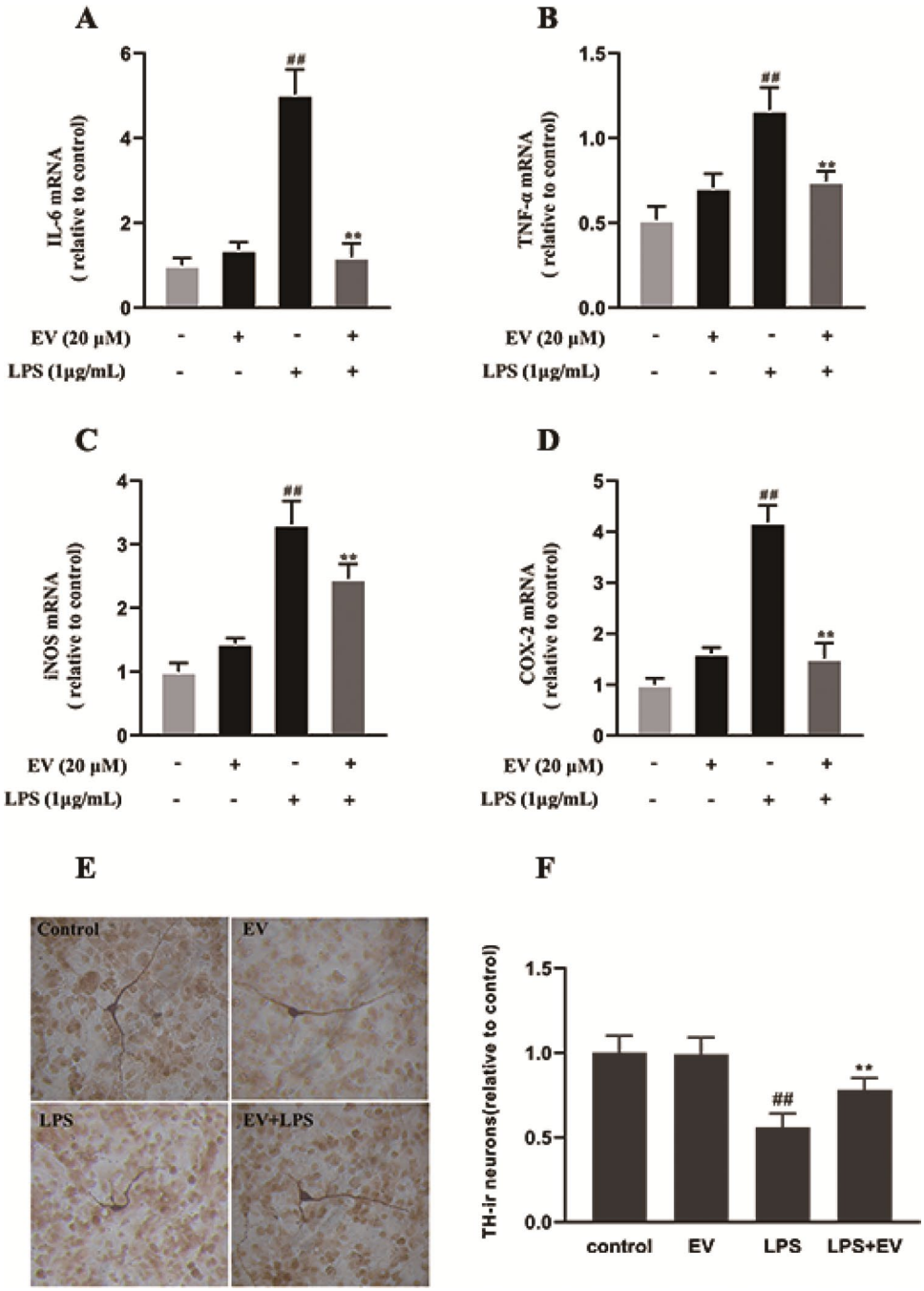


**Fig. 8** eV treatment increasing the number of tyrosine hydroxylase (TH)-positive cells and inhibiting the inflammatory response in primary mouse mesencephalic neuron--glia cells. Mesencephalic neuron--glia cells were pretreated with EV (20 μM) for 1 h and then stimulated with LPS for 4 h. The mRNA levels of IL-6 **a**, TNF-α **b**, iNOS **c**, and COX-2 d were examined by quantitative real-time PCR. Cultures were pretreated with EV (20 μM) for 1 h and then stimulated with LPS. Seven days later, LPS-induced neurotoxicity was assessed by representative immunostaining images **a**, the number of tyrosine hydroxylase (TH)-positive cells **b**. The values are presented as the mean ± SEM ($n = 5$ in each group). $^{\#\#}p < 0.01$ compared to the untreated group. $^{**}p < 0.01$ versus the LPS-treated group

after LPS treatment (Fig. 8e). As expected, EV could abolish this phenomenon (Figs. 8e and 9).

## Discussion

The current findings indicated that EV exerts anti-inflammatory effects by decreasing the production of proinflammatory factor (IL-6 and TNF-α) and enzyme (iNOS and COX-2). The mechanism underlying this process involves the activation of the AKT/Nrf-2/HO-1 signaling pathways and inhibition of the NF-κB pathway. These results highlight EV as a potential drug candidate in neuroinflammation because of its anti-inflammatory effect through activating the AKT/Nrf-2/HO-1 pathway and inhibiting the NF-κB pathway (Fig. 8).

Neurodegenerative diseases are generally associated with oxidative stress, mitochondrial dysfunction (Lin and Beal 2006), excitatory toxins (Fletcher et al. 2017), and inflammation (Amor et al. 2010). The latest research is looking for new causes, such as obesity (Mazon et al. 2017), sleep disorders (Iranzo 2016), and environmental neurotoxin exposure

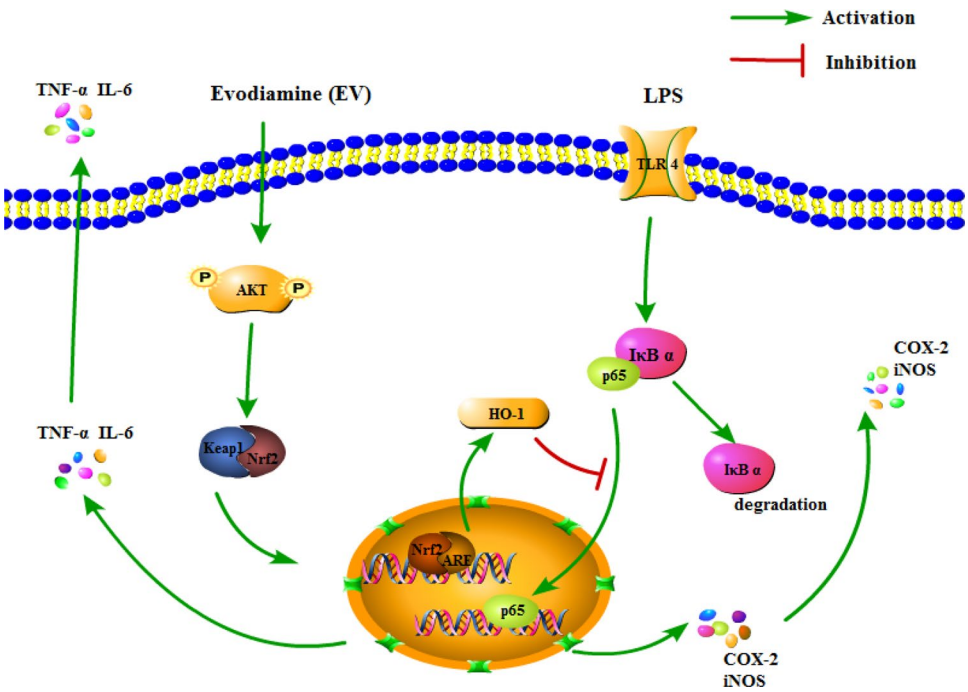


**Fig. 9** Graphical abstract summarizing the anti-inflammatory effects of EV on LPS-induced BV-2 cells via regulation of the AKT/Nrf-2/HO-1/NF-κB signaling pathways

(Cannon and Greenamyre 2011). Many neuropathological conditions are accompanied by microglia overactivation due to the inflammatory response. Under normal circumstances, microglia ensure the structural integrity of the CNS, but continuous overactivation leads to irreversible nerve damage and chronic neurodegenerative diseases. Activation of microglia is accompanied by the production of proinflammatory mediators (iNOS, COX-2, IL-6, and TNF-α), which in turn induce neuronal dysfunction by activating microglia in the brain, interfering with neuronal homeostasis and disrupting the neuronal milieu(Bedi et al. 2013; Bilbo 2010).

LPS is a bacterial endotoxin that is frequently used to induce neuroinflammatory models. Studies have shown that LPS in the brain binds to CD14 receptors on microglial membranes, leading to activation of microglia, further inducing inflammation in the brain, producing neurotoxic substances, and mediating neuronal damage (Herrera et al. 2000; Martins 2015; Qin et al. 2007). EV is an important alkaloid component in Wusong. A large number of studies have shown that EV has many pharmacological effects, such as antitumor, anti-inflammatory, analgesic, antibacterial, endocrine, and hypoglycemic effects (Huang et al. 2015). EV is able to cross the blood–brain barrier (BBB) (Zhang et al. 2018; Zhao et al. 2015). However, no findings have shown whether EV exerts the same neuroprotective effect on BV-2 cells, and the underlying mechanisms remain unclear.

In this study, the BV-2 microglial cell line was used to examine the molecular mechanisms and anti-neuroinflammatory effects of EV in vitro. These cells are not only highly purified but also similar in morphology, phenotype, and functional characteristics to primary cultured microglia (Huang et al. 2018; Mrvova et al. 2015). Besides, to elucidate whether EV's neuroprotective activity involves an anti-inflammatory function, the effect of EV on LPS-induced damage to dopaminergic neurons was investigated in a primary mesencephalic neuron/glia mixed culture (Fu et al. 2015; Jeohn et al. 2002; Tran et al. 2019). It was found that EV attenuated the LPS-induced loss of TH-ir neurons in a primary mesencephalic neuron/glia mixed culture.

NF-κB is a nuclear transcriptional activator that has been studied in recent years. During inflammation, NF-κB regulates the expression of inflammatory mediators (such as TNF-α, IL-6, iNOS, and COX-2). Under physiological conditions, the NF-κB phosphorylation site is blocked by IκB α and is in an inactive state. In various inflammatory lesions, after the upstream IKK kinase degrades IκB α, the nuclear localization signal of P50 is exposed, and NF-κB p65 is rapidly transferred into the nucleus. NF-κB p65 recognizes specific DNA sequences, binds to the IκB α site on the promoter region or enhancer of certain inflammatory factor genes, initiates transcription of related genes, induces overexpression of various cytokines, and further activates NF-κB, thereby amplifying the inflammatory cascade(Chun et al. 2014). The present study concluded that EV activated IκBα and inhibited the activation of NF-κB, thereby down-regulating the secretion of proinflammatory factors and the neuroinflammatory response.

AKT, a serine/threonine kinase, regulates the release of inflammatory factors and has been confirmed to play a vital role in various disease models, such as hypoxic ischemic encephalopathy (Chang and Kong 2019), acute lung injury (Yan et al. 2018), and hepatic ischemia–reperfusion injury

(Chen et al. 2017). Based on these studies, it was hypothesized that EV also affects the inflammatory response through phosphorylation of AKT in LPS-induced BV-2 cells. Western blot results showed that EV promoted the phosphorylation of AKT, which indicated that EV ameliorates the neuroinflammatory response by activating the AKT pathway. Numerous studies have shown that Nrf2 is a key regulator in maintaining redox balance, especially when PI3K-AKT is continuously activated. The activated PI3K-AKT pathway enhances the accumulation of Nrf2 in the nucleus, allowing Nrf2 to express antioxidant, anti-inflammatory, and antiapoptotic genes. These results showed that EV promoted Nrf2 translocation into the nucleus by activating the AKT pathway.

Heme oxygenase-1 (HO-1) is one of the most widely distributed antioxidant enzymes in the body, catalyzes the metabolism of heme to biliverdin, iron ions, and carbon monoxide, and exerts anti-inflammatory effects. Studies have indicated that HO-1 is regulated by the Nrf2 signaling pathway (Chen et al. 2003; Pittala et al. 2013). Under physiological conditions, through Keap1, Nrf2 is sequestered in the cytosol and is targeted for proteasomal degradation. In the presence of reactive oxygen species (ROS) or electrophilic species, Nrf2 is released from Keap1 and translocates into the nucleus to activate target gene transcription, including HO-1(Nguyen et al. 2009). In this study, BV-2 cells were treated with Nrf-2 and AKT inhibitors, and it was found that EV activated the AKT/Nrf2/HO-1 signaling pathways in BV-2 cells. Furthermore, treatment with an HO-1 inhibitor partly inhibited LPS-induced activation of the NF-κB pathway and reversed the anti-inflammatory effects of EV, which suggests that EV exerts anti-neuroinflammatory effects by activating the AKT/Nrf2/HO-1/NF-κB signaling pathways. This study only investigated the effect of EV on murine microglial line BV-2 cells. In vivo experiments are also necessary to fully examine the anti-inflammatory effect of EV. Other signaling pathways and molecular mechanisms still need to be discovered.

In conclusion, EV plays an important role in neuroinflammation by activating the AKT/Nrf-2/HO-1/NF-κB signaling pathways in LPS-stimulated BV-2 cells, and EV has a neuroprotective effect on dopaminergic neurons in mesencephalic neuron--glia cells. Previous studies have shown that EV can pass through the BBB (Zhang et al. 2018; Zhao et al. 2015). This indicates that EV exhibits significant neuroprotective properties, providing a potential basis for EV as a therapeutic agent for neurodegenerative diseases.

## Materials and Methods

### Reagents and Chemicals

TRIzol reagent and Cell Counting Kit-8 (CCK-8) were provided by BestBio (Shanghai, China). Trypsin was purchased from MP Biomedicals (Santa Ana, California, USA). Penicillin–streptomycin (PS) solution and phosphate buffered saline (PBS) were supplied by Meilunbio (Dalian, China). IL-6 and TNF-α ELISA kits were procured from Sino Biological (Beijing, China). LPS (*E. coli*, Serotype O55:B5) and Dulbecco's modified Eagle's medium (DMEM) were obtained from Solarbio (Beijing, China). Evodiamine (EV, > 98% purity) was purchased from Yuan ye Biotech (Shanghai, China). Fetal bovine serum (FBS) and dimethyl sulfoxide (DMSO) were obtained from Genetimes (Shanghai, China). MK2206 dihydrochloride (an AKT inhibitor), retinoic acid (RA, a Nrf-2 inhibitor), and tin protoporphyrin-IX (SnPP-IX, a HO-1 inhibitor) were purchased from Santa Cruz (CA, USA).

### Cell Culture and Treatment

The mouse microglial cell line BV-2 was provided by the Cell Culture Center in the Chinese Academy of Medical Sciences (Beijing, China). BV-2 cells were plated in DMEM containing 10% FBS and cultured in an incubator containing 5% $CO_2$ at 37 °C. The medium was replaced every day, and the cells were passaged every two days by trypsin digestion (0.05%). Once the density reached approximately 80%, BV-2 cells were cultured in 24-well, 12-well, or 96-well plates for subsequent experiments. The medium was changed to incomplete medium (without serum) 4 h before the cells were treated with LPS or EV. Pretreatment of BV-2 cells was performed with various concentrations (10 and 20 μM) of EV (in 0.1% DMSO solution) for 1 h. Then, BV-2 cells were treated with LPS (1 μg/mL) for specific periods (12 h, 6 h or 1 h).

### Cell Viability Assay

Cell viability was detected using a CCK-8 assay kit (Beyotime Inst. Biotech, Beijing, China). Briefly, BV-2 cells were cultured in 96-well plates at an initial density of $10^4$ cells per well for one day and then incubated with or without EV at concentrations of 0, 2.5, 5, 10, or 20 μM in 0.1% DMSO for 24 h. After that, the supernatant was discarded, and CCK-8 solution was added for 2 h. Absorbance at 450 nm was measured using a spectrophotometer (Cole-Parmer, Chicago, IL, USA).

### Quantitative Real-Time PCR

Total RNA was extracted using TRIzol reagent (BestBio, Shanghai, China) according to the instructions and reverse transcribed to create cDNA templates with the cDNA synthesis kit (Thermo Scientific, Waltham, MA, USA). The cDNA templates were then amplified by the Rapid SYBR® Green qPCR kit to assess mRNA levels of various genes,

and each sample was performed in triplicate. The primer sequences (Chen et al. 2017; He et al. 2018) evaluated are shown in Table 1.

## Western Blotting Analysis

Cells were collected and lysed with P0013B RIPA lysis buffer (Beyotime Inst. Biotech, Beijing, China) containing 10% phenylmethylsulfonyl fluoride (PMSF, Sigma-Aldrich, Shanghai, China). The nucleoproteins of BV-2 cells were obtained using a nuclear extraction kit (Epigentek, Farmingdale, NY, USA). The protein concentration was quantified using a bicinchoninic acid (BCA) protein assay kit (Beyotime Biotech, Shanghai, China). Protein samples (40 μg) were subjected to 12% SDS-PAGE and then transferred to polyvinylidene difluoride (PVDF) membranes (Beyotime Biotech, Shanghai, China). Then, the membranes were incubated with 5% skim milk at approximately 23 °C for 2 h, followed by incubation with primary antibodies against iNOS (1:2000), COX-2 (1:2000), Nrf2 (1:3000), AKT (1:3000), NF-κB p65 (1:4000), IκB (1:3000), HO-1 (1:4000), phospho-AKT (1:3000), phospho-NF-κB p65 (1:2000) (Cell Signaling Technology, MA, USA), phospho-IκB (1:2000), β-actin (1:4000), and PCNA (1:4000) (Santa Cruz, CA, USA) at 4 °C for 24 h. The PVDF membranes were then incubated with goat anti-rabbit (1:5000) or goat anti-mouse (1:5000) secondary antibodies in skim milk for 2 h at room temperature. ECL Western blot detection reagents (Millipore, MA, USA) were used to visualize protein expression, and the blots were quantified by ImageJ (National Institutes of Health, Bethesda, MD, USA).

## Enzyme-Linked Immunosorbent Assay (ELISA)

BV-2 cells were digested with 0.05% trypsin and cultured in 12-well plates ($5 \times 10^5$ cells per well). When the density reached approximately 80%, the cells were pretreated with EV (10 and 20 μM) for 1 h and then exposed to LPS (1 μg/mL) for 24 h. Cytokine determination was performed in strict accordance with the instructions of the ELISA kits.

## Mouse Mesencephalic Neuron--Glia Cultures

Ten fetal Wistar rats between 14 and 16 days old were collected, and the whole brains were placed in Hank's balanced salt solution containing $Ca^{2+}$ and $Mg^{2+}$. After removing the meninges and blood vessels, the cells were separated by digestion with 0.25% trypsin and centrifugation. The supernatant was discarded, and an appropriate amount of complete medium (MEM containing 10% FBS, 10% horse serum, 2 mM L-glutamine, 1 mM sodium pyruvate, 100 μM non-essential amino acids, 50 U/mL penicillin, and 50 μg/mL streptomycin) was added. After counting the cells, an appropriate amount of medium was added to adjust the number of cells, and $2 \times 10^5$ cells per well were seeded. The 24-well plate was placed in an incubator at 37 °C and 5% $CO_2$. A half-volume exchange of medium was performed every two days, and the cells were used for experiments on the seventh day.

## Tyrosine Hydroxylase Immunocytochemical Analysis

The mouse mesencephalic neuron--glia cultures were fixed and processed for immunostaining as described previously (Fu et al. 2015). The primary antibody is rabbit polyclonal anti-tyrosine hydroxylase (TH). To determine cell numbers, TH-positive cells were counted by three researchers blind to the experimental design, and the average of these scores was reported.

## Statistical Analysis

The data were acquired through repeated experiments and are presented as the mean ± SEM. Statistical analysis was carried out by SPSS 20.0 software (SPSS Inc., Chicago, IL, USA). Significance between different groups was evaluated by analysis of variance (ANOVA), and minor differences in mean values between results were determined by least significant difference (LSD) tests. A value of $p < 0.05$ or $p < 0.01$ indicated a significant difference.

**Table 1** The primer sequences of TNF-α, IL-6, iNOS, COX-2, and β-actin

| Gene | Sequences | Length (bp) |
|---|---|---|
| IL-6 | (F) 5′-CCAGAAACCGCTATGAAGTTCC-3′<br>(R) 5′-GTTGGGAGTGGTATCCTCTGTGA-3′ | 138 |
| TNF-α | (F) 5′-GCAACTGCTGCACGAAATC-3′<br>(R) 5′-CTGCTTGTCCTCTGCCCAC -3′ | 136 |
| iNOS | (F) 5′-GAACTGTAGCACAGCACAGGAAAT-3′<br>(R) 5′-CGTACCGGATGAGCTGTGAAT-3′ | 158 |
| COX-2 | (F) 5′-CAGTTTATGTTGTCTGTCCAGAGTTTC-3′<br>(R) 5′-CCAGCACTTCACCCATCAGTT-3′ | 127 |
| β-actin | (F) 5′-GTCAGGTCATCACTATCGGCAAT-3′<br>(R) 5′-AGAGGTCTTTACGGATGTCAACGT-3′ | 147 |

**Acknowledgements** This work was funded by National Natural Science Foundation of China (project No. 31772547, 31702211), Jilin Scientific and Technological Development Program (project No. 20170623083-04TC), and JLU Science and Technology Innovative Research Team (project No. 201910183X588, 201910183811).

**Author Contributions** TM, SF, DH, and GH performed most of the experiments, analyzed the results, and wrote the manuscript. DL conceived and designed this study and analyzed the data. They were involved in all aspects of the study read and modified the manuscript. XG, YZ, BH, JD, AZ, and YS also participated in the research. All the authors read and approved the final manuscript.

## Compliance with Ethical Standards

**Conflicts of interest** The authors declare no conflict of interest.

**Ethical Approval** This article does not contain any studies with human participants or animals performed by any of the authors. The study complies with current ethical consideration.

## References

Amor S, Puentes F, Baker D, van der Valk P (2010) Inflammation in neurodegenerative diseases. Immunology 129:154–169. https://doi.org/10.1111/j.1365-2567.2009.03225.x

Bedi SS, Smith P, Hetz RA, Xue H, Cox CS (2013) Immunomagnetic enrichment and flow cytometric characterization of mouse microglia. J Neurosci Methods 219:176–182. https://doi.org/10.1016/j.jneumeth.2013.07.017

Bilbo SD (2010) Early-life infection is a vulnerability factor for aging-related glial alterations and cognitive decline. Neurobiol Learn Mem 94:57–64. https://doi.org/10.1016/j.nlm.2010.04.001

Cai QY, Li WR, Wei JJ, Mi SQ, Wang NS (2014) Antinociceptive activity of aqueous and alcohol extract of evodia rutaecarpa. Indian J Pharm Sci 76:235–239

Cannon JR, Greenamyre JT (2011) The role of environmental exposures in neurodegeneration and neurodegenerative diseases. Toxicol Sci 124:225–250. https://doi.org/10.1093/toxsci/kfr239

Chang Y, Kong R (2019) Ganoderic acid A alleviates hypoxia-induced apoptosis, autophagy, and inflammation in rat neural stem cells through the PI3K/AKT/mTOR pathways. Phytother Res 33:1448–1456. https://doi.org/10.1002/ptr.6336

Chen G et al. (2017) Galangin reduces the loss of dopaminergic neurons in an LPS-evoked model of Parkinson's disease in rats. Int J Mol Sci 19 doi:10.3390/ijms19010012

Chen YH, Yet SF, Perrella MA (2003) Role of heme oxygenase-1 in the regulation of blood pressure and cardiac function. Exp Biol Med (Maywood) 228:447–453. https://doi.org/10.1177/153537020322805-03

Chun JM, Nho KJ, Kim HS, Lee AY, Moon BC, Kim HK (2014) An ethyl acetate fraction derived from Houttuynia cordata extract inhibits the production of inflammatory markers by suppressing NF-small ka, CyrillicB and MAPK activation in lipopolysaccharide-stimulated RAW 264.7 macrophages BMC complement. Altern Med 14:234. https://doi.org/10.1186/1472-6882-14-234

Fletcher EV et al (2017) Reduced sensory synaptic excitation impairs motor neuron function via Kv2.1 in spinal muscular atrophy. Nat Neurosci 20:905–916. https://doi.org/10.1038/nn.4561

Fu SP et al (2015) Anti-inflammatory effects of BHBA in both in vivo and in vitro Parkinson's disease models are mediated by GPR109A-dependent mechanisms. J Neuroinflamm 12:9. https://doi.org/10.1186/s12974-014-0230-3

He D et al. (2018) Tubeimoside I protects dopaminergic neurons against inflammation-mediated damage in lipopolysaccharide (LPS)-evoked model of Parkinson's disease in rats. Int J Mol Sci 19. doi:10.3390/ijms19082242

Herrera AJ, Castano A, Venero JL, Cano J, Machado A (2000) The single intranigral injection of LPS as a new model for studying the selective effects of inflammatory reactions on dopaminergic system. Neurobiol Dis 7:429–447. https://doi.org/10.1006/nbdi.2000.0289

Hirsch EC, Hunot S (2009) Neuroinflammation in Parkinson's disease: a target for neuroprotection? Lancet Neurol 8:382–397. https://doi.org/10.1016/S1474-4422(09)70062-6

Hu CY, Wu HT, Su YC, Lin CH, Chang CJ, Wu CL (2017) Evodiamine exerts an anti-hepatocellular carcinoma activity through a WWOX-dependent pathway molecules 22. doi:10.3390/molecules22071175

Huang B et al (2018) Polydatin Prevents Lipopolysaccharide (LPS)-Induced Parkinson's Disease via Regulation of the AKT/GSK-3beta-Nrf2/NF-kappaB Signaling. Axis Front Immunol 9:2527. https://doi.org/10.3389/fimmu.2018.02527

Huang J et al (2015) Antiproliferation effect of evodiamine in human colon cancer cells is associated with IGF-1/HIF-1alpha down-regulation. Oncol Rep 34:3203–3211. https://doi.org/10.3892/or.2015.4309

Hurley SD, O'Banion MK, Song DD, Arana FS, Olschowka JA, Haber SN (2003) Microglial response is poorly correlated with neurodegeneration following chronic, low-dose MPTP administration in monkeys. Exp Neurol 184:659–668. https://doi.org/10.1016/S0014-4886(03)00273-5

Iranzo A (2016) Sleep in Neurodegenerative Diseases. Sleep Med Clin 11:1–18. https://doi.org/10.1016/j.jsmc.2015.10.011

Jeohn GH et al (2002) p38 MAP kinase is involved in lipopolysaccharide-induced dopaminergic neuronal cell death in rat mesencephalic neuron-glia cultures. Ann N Y Acad Sci 962:332–346. https://doi.org/10.1111/j.1749-6632.2002.tb04078.x

Jewett M, Jimenez-Ferrer I, Swanberg M (2017) Astrocytic expression of GSTA4 is associated to dopaminergic neuroprotection in a Rat 6-OHDA model of Parkinson's disease Brain Sci 7. doi:10.3390/brainsci7070073

Khanam H, Ali A, Asif M, Shamsuzzaman (2016) Neurodegenerative diseases linked to misfolded proteins and their therapeutic approaches: a review. Eur J Med Chem 124:1121–1141. https://doi.org/10.1016/j.ejmech.2016.08.006

Liddelow SA et al (2017) Neurotoxic reactive astrocytes are induced by activated microglia. Nature 541:481–487. https://doi.org/10.1038/nature21029

Lin MT, Beal MF (2006) Mitochondrial dysfunction and oxidative stress in neurodegenerative diseases. Nature 443:787–795. https://doi.org/10.1038/nature05292

Martins IJ (2015) Overnutrition determines LPS regulation of mycotoxin induced neurotoxicity in neurodegenerative diseases. Int J Mol Sci 16:29554–29573. https://doi.org/10.3390/ijms161226190

Mazon JN, de Mello AH, Ferreira GK, Rezin GT (2017) The impact of obesity on neurodegenerative diseases. Life Sci 182:22–28. https://doi.org/10.1016/j.lfs.2017.06.002

Miklossy J, Doudet DD, Schwab C, Yu S, McGeer EG, McGeer PL (2006) Role of ICAM-1 in persisting inflammation in Parkinson disease and MPTP monkeys. Exp Neurol 197:275–283. https://doi.org/10.1016/j.expneurol.2005.10.034

Mohan V, Agarwal R, Singh RP (2016) A novel alkaloid, evodiamine causes nuclear localization of cytochrome-c and induces apoptosis independent of p53 in human lung cancer cells. Biochem Biophys Res Commun 477:1065–1071. https://doi.org/10.1016/j.bbrc.2016.07.037

Mrvova N, Skandik M, Kuniakova M, Rackova L (2015) Modulation of BV-2 microglia functions by novel quercetin pivaloyl ester. Neurochem Int 90:246–254. https://doi.org/10.1016/j.neuint.2015.09.005

Nguyen T, Nioi P, Pickett CB (2009) The Nrf2-antioxidant response element signaling pathway and its activation by oxidative stress. J Biol Chem 284:13291–13295. https://doi.org/10.1074/jbc.R900010200

Norden DM, Muccigrosso MM, Godbout JP (2015) Microglial priming and enhanced reactivity to secondary insult in aging, and traumatic CNS injury, and neurodegenerative disease. Neuropharmacology 96:29–41. https://doi.org/10.1016/j.neuropharm.2014.10.028

Pittala V, Salerno L, Romeo G, Modica MN, Siracusa MA (2013) A focus on heme oxygenase-1 (HO-1) inhibitors. Curr Med Chem 20:3711–3732. https://doi.org/10.2174/0929867311320300003

Qin L et al (2007) Systemic LPS causes chronic neuroinflammation and progressive neurodegeneration. Glia 55:453–462. https://doi.org/10.1002/glia.20467

Rosa AI et al (2018) Tauroursodeoxycholic acid improves motor symptoms in a mouse model of Parkinson's disease. Mol Neurobiol 55:9139–9155. https://doi.org/10.1007/s12035-018-1062-4

Spires-Jones TL, Attems J, Thal DR (2017) Interactions of pathological proteins in neurodegenerative diseases. Acta Neuropathol 134:187–205. https://doi.org/10.1007/s00401-017-1709-7

Tran C et al. (2019) Sphingosine 1-phosphate but not Fingolimod protects neurons against excitotoxic cell death by inducing neurotrophic gene expression in astrocytes. J Neurochem e14917. doi:10.1111/jnc.14917

Wang XX et al (2013) Quinolone alkaloids with antibacterial and cytotoxic activities from the fruits of Evodia rutaecarpa. Fitoterapia 89:1–7. https://doi.org/10.1016/j.fitote.2013.04.007

Wei J, Ching LC, Zhao JF, Shyue SK, Lee HF, Kou YR, Lee TS (2013) Essential role of transient receptor potential vanilloid type 1 in evodiamine-mediated protection against atherosclerosis. Acta Physiol (Oxf) 207:299–307. https://doi.org/10.1111/apha.12005

Wei L, Jin X, Cao Z, Li W (2016) Evodiamine induces extrinsic and intrinsic apoptosis of ovarian cancer cells via the mitogen-activated protein kinase/phosphatidylinositol-3-kinase/protein kinase B signaling pathways. J Tradit Chin Med 36:353–359. https://doi.org/10.1016/s0254-6272(16)30049-8

Wu JY et al (2013) Topoisomerase I inhibitor evodiamine acts as an antibacterial agent against drug-resistant Klebsiella pneumoniae. Planta Med 79:27–29. https://doi.org/10.1055/s-0032-1327925

Yan J et al (2018) Nrf2 protects against acute lung injury and inflammation by modulating TLR4 and Akt signaling. Free Radic Biol Med 121:78–85. https://doi.org/10.1016/j.freeradbiomed.2018.04.557

Yu H, Jin H, Gong W, Wang Z, Liang H (2013) Pharmacological actions of multi-target-directed evodiamine. Molecules 18:1826–1843. https://doi.org/10.3390/molecules18021826

Zhang YN, Yang YF, Yang XW (2018) Blood-brain barrier permeability and neuroprotective effects of three main alkaloids from the fruits of Euodia rutaecarpa with MDCK-pHaMDR cell monolayer and PC12 cell line. Biomed Pharmacother 98:82–87. https://doi.org/10.1016/j.biopha.2017.12.017

Zhao Z, Gong S, Wang S, Ma C (2015) Effect and mechanism of evodiamine against ethanol-induced gastric ulcer in mice by suppressing Rho/NF-small ka CyrillicB pathway. Int Immunopharmacol 28:588–595. https://doi.org/10.1016/j.intimp.2015.07.030

Zhou P et al (2019) Evodiamine inhibits migration and invasion by Sirt1-mediated post-translational modulations in colorectal cancer. Anticancer Drugs 30:611–617. https://doi.org/10.1097/CAD.0000000000000760